reactions

MDPI

Review

Ir-Catalyzed *ortho*-C-H Borylation of Aromatic C(sp^2)-H Bonds of Carbocyclic Compounds Assisted by *N*-Bearing Directing Groups

Hamad H. Al Mamari

Department of Chemistry, College of Science, Sultan Qaboos University, P.O. Box 36, Al-Khod, Muscat 123, Oman; halmamari@squ.edu.om

Abstract: C-H borylation is a powerful strategy for the construction of C-B bonds due to the synthetic versatility of C-B bonds. Various transition metals affect the powerful functionalization of C-H bonds, of which Ir is the most common. Substrate-directed methods have enabled directed Ir-catalyzed C-H borylation at the *ortho* position. Amongst the powerful directing groups in Ir-catalyzed C-H borylation are N-containing carbocyclic systems. This review covers substrate-directed Ir-catalyzed *ortho*-C-H borylation of aromatic C(sp2)-H bonds in N-containing carbocyclic compounds, such as anilines, amides, benzyl amines, hydrazones, and triazines.

Keywords: Ir-catalysis; C-H functionalization; C-H borylation; directing groups; *N*-bearing directing groups; directed C-H borylation

check for updates

Citation: Al Mamari, H.H. Ir-Catalyzed *ortho*-C-H Borylation of Aromatic C(sp^2)-H Bonds of Carbocyclic Compounds Assisted by *N*-Bearing Directing Groups. *Reactions* **2024**, *5*, 318–337. https://doi.org/10.3390/reactions5020016

Academic Editor: Shiuh-Tzung Liu

Received: 29 February 2024
Revised: 4 April 2024
Accepted: 25 April 2024
Published: 1 May 2024

1. Introduction

Functionalization of inert C-H bonds has emerged as a powerful strategy for making functional and versatile bonds [1–7]. Transformation of inert non-functional C-H bonds into reactive functional bonds is an attractive chemically powerful strategy. Thus, the functionalization of C-H bonds should provide rapid access to functionalized molecules from simple starting materials. In this process, step and reaction economies can be achieved by shortening the number of steps in multi-step synthesis, simplifying reaction conditions, or minimizing the need for pre-functionalized reagents. C-H Bond functionalization is typically catalyzed by transition metals. Functionalization of C-H bonds by second-row transition metals, such as Pd [8–11], Rh [12–16], and Ru [17–21], has received widespread attention from the scientific community. Earth-abundant first-row transition metals, ref. [22] such as Ni [23–25], Mn [26,27], Fe [28,29], and Co [30–34], have also been used in the field. Given the ubiquitous nature of C-H bonds in molecules, controlling what C-H bonds are functionalized is a challenge. The issue of regioselectivity or site-selectivity in C-H bond functionalization is a constant target. One approach to solve the issue is the use of directing groups, which include two general types, monodentate and bidentate [35]. The classification depends on the number of Lewis basic atoms that can participate in the functionalization reaction through chelation assistance. Lewis basic atoms coordinate the Lewis acidic metal used in the reaction, hence directing it in proximity to a C-H bond to be cleaved and subsequently functionalized. The formation of cyclometallated complexes or chelates is controlled by ring size, of which five-membered chelates are thermodynamically more stable and thus favored over other ring sizes [36]. Thus, the atom distance between the Lewis basic atom in the directing group and the C-H bond to be functionalized is critical. For the formation of the more common five-membered chelates, the atom distance should be two carbons. Monodentate directing groups possess one Lewis basic atom that allows the formation of a single (typically five-membered) chelate, while bidentate directing groups possess two Lewis basic atoms that facilitate the formation of double or bis-five-membered chelates. In bidentate directing groups, the atom distance

between the first Lewis basic atom and the C-H bond to be functionalized is critical, as noted in monodentate directing groups. In addition, the atom distance between the two Lewis basic atoms constituting the bidentate directing group is important as well [37]. Many monodentate and bidentate directing groups have been established in the field of C-H bond functionalization [10–12]. A wide range of functionalization reactions of C-H bonds by "direction" or chelation assistance are possible based on the catalysis of various transition metals.

Conversion of C-H bonds into C-B bonds is a unique type of C-H bond functionalization [38–44]. This is based on the synthetic versatility and utility of alkyl and aryl boronates in organic synthesis. C-B bonds can be transformed into various bonds with a wide range of functional groups, such as amines, alcohols/phenols, aryl halides, and biaryls [45]. The synthetic versatility of C-B bonds allows C-H borylation to be used as a unique and powerful C-H functionalization strategy. As noted for C-H bond functionalization as a whole, controlling the pressing issue of regioselectivity or site-selectivity is a constant target.

C-H bond borylation is a unique type of C-H bond functionalization reaction that converts inert C-H bonds into C-B bonds. Metal-catalyzed C-H borylation is made possible by the catalysis of various transition metals, such as Ir [38–44], Co [46–48], Ni [49], and Fe [50].

As noted in C-H bond functionalization, controlling the pressing issue of regioselectivity or site-selectivity is a constant goal. Generally, the Ir-catalyzed C-H borylation reaction of carbocyclic compounds is sterically driven [38–44]. Electronic effects can also play a role in the site-selectivity of C-H borylation of heterocycles.

The regioselectivity or site-selectivity of C-H borylation can be controlled using directing groups *via* chelation assistance (Scheme 1) [51,52]. Directing groups containing Lewis basic atoms (*vide supra*) in substrate, **1** can direct C-H borylation to take place selectively at the *ortho* position to give *ortho*-borylated product **2** (Scheme 1).

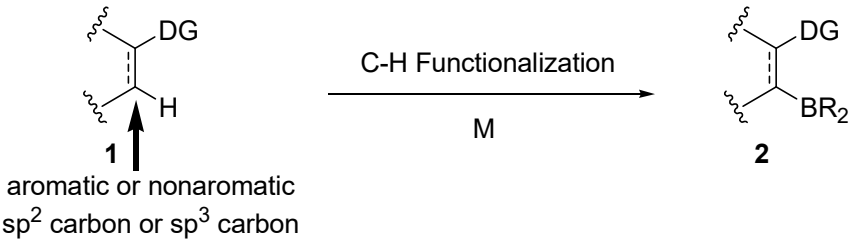

Scheme 1. General representation of directed C-H borylation.

Substrate-directed C-H borylation is possible with various functional groups, such as ketones [53], ethers [54], sulfides [55], and phenols [56–58].

Several Ir precatalysts can be used in Ir-catalyzed C-H borylation. The following Ir catalysts are used: $[Ir(OMe)(COD)]_2$, $[Ir(OH)(COD)]_2$, $[Ir(OPh)(COD)]_2$, $[Ir(OAc)(COD)]_2$, $[Ir(Cl)(COD)]_2$, $[Ir(COD)_2]BF_4$, $[Ir(COE)_2Cl]_2$, Cp*Ir(PMe_3)(H)(Bpin), (Ind)Ir(COD), (η6-mesitylene)Ir$(Bpin)_3$, and Ir(acac)(cod). The structures of a few of these catalysts are shown below (Figure 1) [42,59].

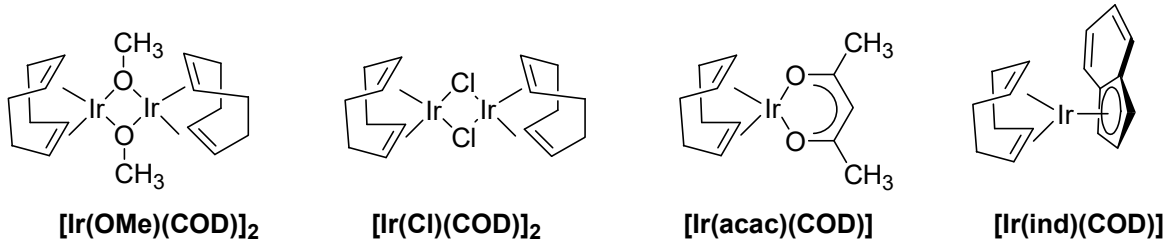

Figure 1. Common Ir precatalysts in Ir-catalyzed C-H borylation.

Various differences are noted between these precatalysts, including their electronic and steric characteristics; their stability, ease of handling and manipulation; and their ability to form active Ir complexes with ligands. In turn, the ligands used can play a pivotal role in forming Ir complexes capable of catalyzing C-H bond borylation. Examples of bipyridine ligands are shown below (Figure 2) [42]. Ligands L1-L9 represent common bipyridine ligands used or can be used.

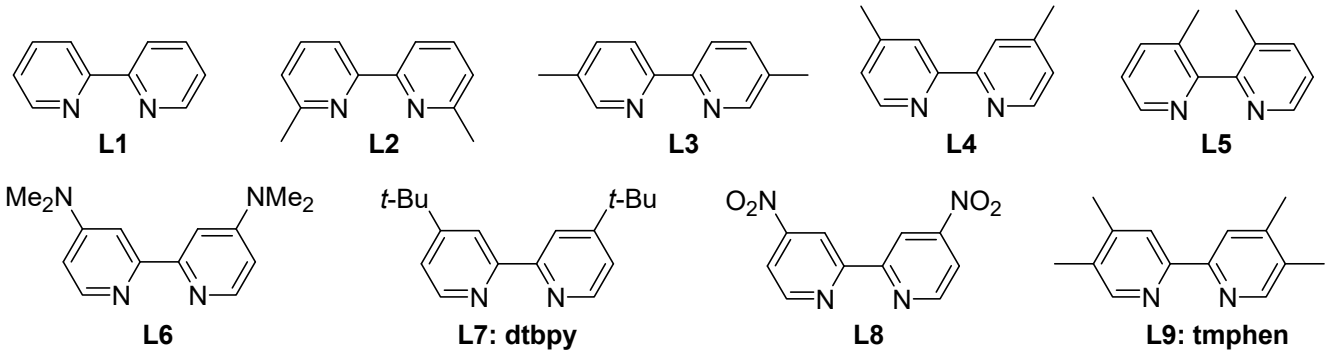

Figure 2. Bipyridine ligands.

By far, $[Ir(OMe)(COD)]_2$ is the most commonly used catalyst due to its air stability, ease of handling, and most efficient capability of forming Ir trisboryl complexes [Ir(Bpin)3(L2)-alkene] where L is dtbpy or tmphen (Figure 3). COE: cyclooctene, Bpin: 4,4,5,5-tetramethyl-1,3,2-dioxaboro-lanyl [60].

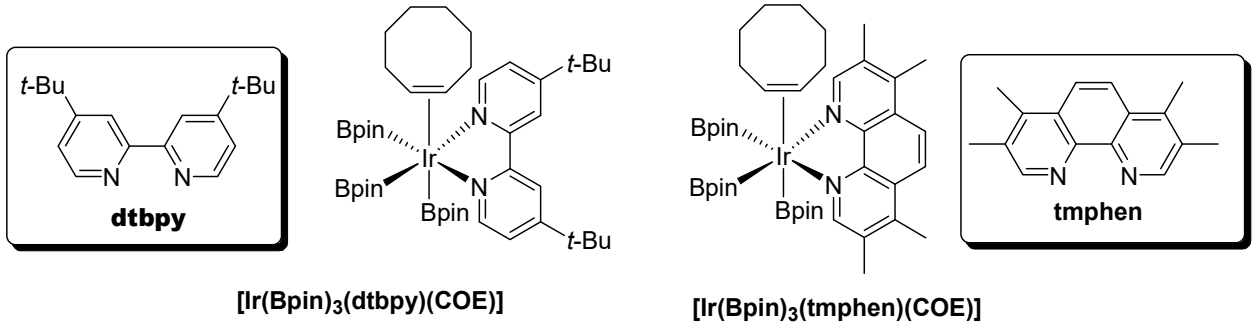

Figure 3. Ability of $[Ir(OMe)(COD)]_2$ to form Ir trisboryl complexes.

The mechanism of Ir-catalyzed C-H borylation has been studied [60,61]. Based on these findings, an Ir trisporyl complex **A** is formed upon treatment of an Ir precatalyst, such as the most commonly used $[Ir(OMe)(COD)]_2$, with a ligand typically dtbpy (Scheme 2) [60–62]. Subsequent treatment of the Ir trisboryl complex with a carbocyclic compound or hydrocarbon gives intermediate **B**. A borylated carbocyclic compound is then released with concomitant formation of intermediate **C**. The addition of B_2pin_2 or H-BPin forms intermediate **D**, which subsequently regenerates the starting Ir tisboryl complex **A** in the catalytic cycle (Scheme 2).

Typically, C-H borylation is sterically driven [38–44]. Directing the reaction to regioselectively occur at an *ortho* position concerning a functional group is not straightforward [51,52]. *ortho*-Directing groups, including monodentate and bidentate directing groups typically used in directed C-H bond functionalization catalyzed by other transition metals may not simply be used to direct Ir-catalyzed C-H borylation reactions. A key challenge in *ortho*-C-H borylation is directing the reaction to occur regioselectively at the *ortho*-position. Coordination between the Lewis acidic Ir center and the Lewis basic directing group utilizing a vacant site in the metal center can be problematic. When a directing group coordinates with the Ir center in the 16-electron [Ir] trisboryl species **3**, an

Ir complex **4** is formed that does not advance the reaction forward to the desired *ortho*-C-H borylation (Scheme 3) [60,61].

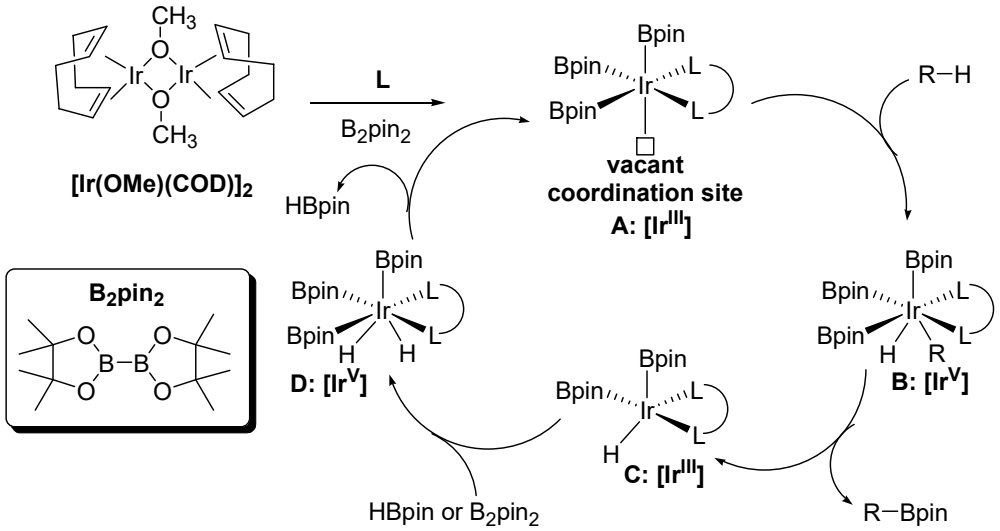

Scheme 2. A plausible general mechanism of Ir-catalyzed C-H borylation.

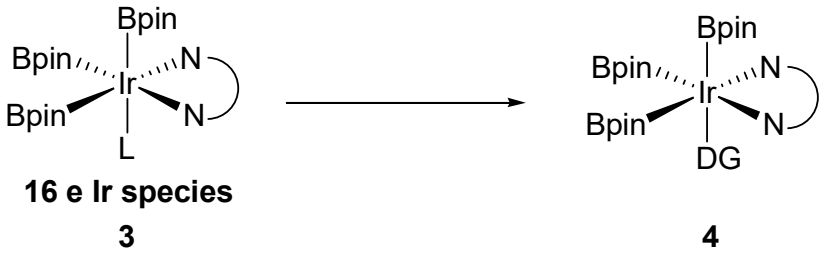

Scheme 3. Possible coordination between the Ir trisboryl complex and directing groups.

Another problem may arise when ligands coordinate with the Ir trisboryl complex rendering the resultant Ir species inactive towards directed ortho-selective C-H borylation. This event could be notable when the ligand is strongly coordinating.

To overcome these problems, a chelate-directed C-H borylation strategy could be used [51,52]. The strategy relies on coordination between the Lewis acidic Ir center and the Lewis basic directing group as well as a judicious choice of the ligand. The latter is critical for the formation of vacant sites in the Ir center [60,61].

Another strategy to circumvent problems of Ir-catalyzed *ortho*-C-H borylation is to use monodentate or hemi-labile ligands to form a transient vacant coordination site on the Ir center. This strategy specifically circumvents the complications that arise when Lewis basic directing groups coordinate with Ir. The hemi-lability of ligands creates vacant coordination sites on the Ir center setting the stage for subsequent C-H bond cleavage [51].

Another solution for successfully directed C-H borylation is the use of a solid/silica-supported compact monophosphine–Ir system, such as Silica-SMAP–Ir developed by Sawmaura et al. The strategy has been employed to affect *ortho*-Ir-catalyzed C-H borylation of various functional groups [63–68].

The most common [Ir] precatalyst is the commercially available (1,5-cyclooctadiene)-(methoxy)iridium(I) dimer [Ir(OMe)((COD)]$_2$, which upon treatment with ligands and bis(pinacolato)diboron, B_2pin_2, can give rise to a 14-electron [Ir] species 5 (Scheme 4). Directing groups (represented by **6**) can coordinate with the 14-electron [Ir] species **5** through vacant sites on the metal center. Upon Lewis base–Lewis acid interactions between the directing group and the Lewis acidic metal center, the 16-electron [Ir] species **7** should form. The Lewis base–Lewis acid coordination brings the Ir center in proximity to an

ortho C-H in the directing group, thus facilitating C-H bond cleavage and forming the intermediate [Ir] species **8**. Subsequently, the *ortho* position in the directing group is borylated with the Bpin moiety from the Ir center to give rise to *ortho*-borylated product **9** (Scheme 4) [59–62].

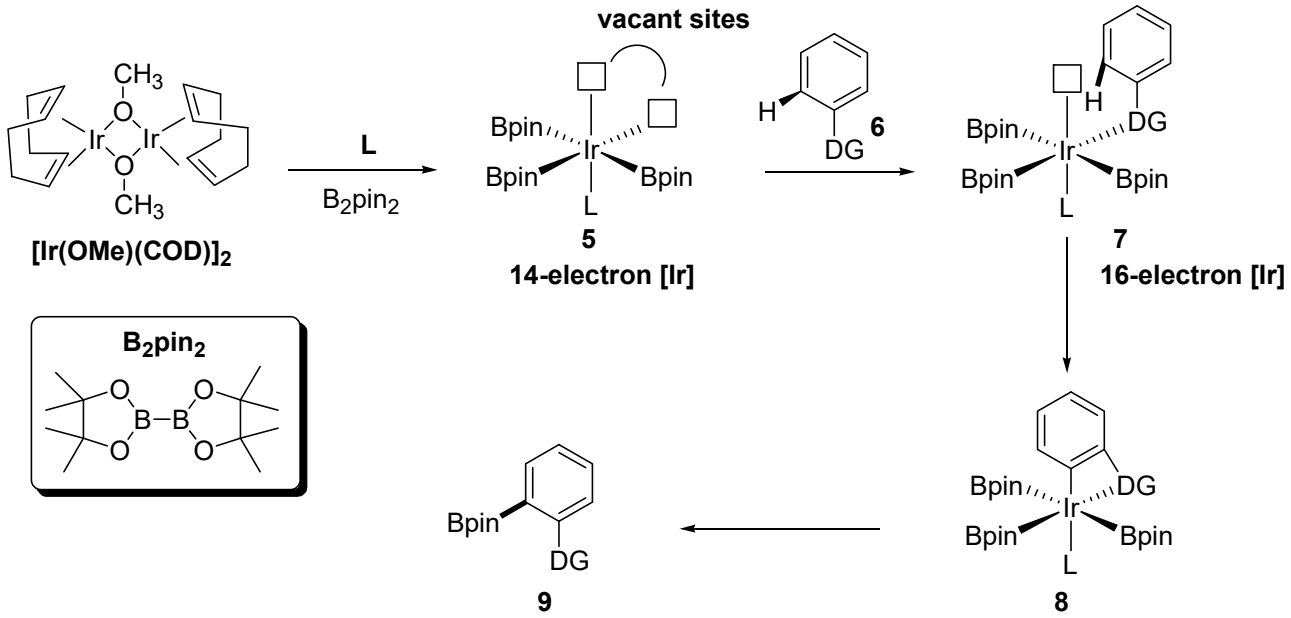

Scheme 4. Envisaged directing role in the substrate-directed Ir-catalyzed C-H *ortho*-borylation of carbocycles.

This review focuses on Ir-catalyzed *ortho*-C-H borylation of aromatic C(sp^2)-H bond assisted by *N*-bearing directing groups. The review covers research findings on the topic from 2012 to 2023.

2. Discussion

2.1. Anilines

In 2012, the NHBoc group was reported to function as a directing group in Ir-catalyzed *ortho*-C-H borylation of N-Boc-protected anilines (**10**, Scheme 5) [69]. The directed C-H borylation employed $[Ir(OMe)(COD)]_2$ as a precatalyst and B_2pin_2 as a boron source and proceeded with *ortho* selectivity. The reaction proceeded with good functional group tolerance and good yields (Scheme 5). For example, ether and halogens are tolerated as demonstrated by *ortho*-borylated NH-Boc anilines **11a** and **11b,** which were obtained with yields of 96% and 79%, respectively. The use of the cyano group as an electron-withdrawing group was tolerated as noted in borylated product **11c,** which was obtained with a modest 40% yield. The free hydroxyl group was also tolerated as exemplified by borylated hydroxyl NH-Boc protected aniline **11d,** which was obtained with a 78% yield. In addition, carbamates were also tolerated as demonstrated by borylated materials **11e** and **11f,** which were obtained with 44% and 62% yields, respectively (Scheme 3). The reaction reveals good functional group tolerance.

In 2013, Bpin was reported to function as a traceless directing group in Ir-catalyzed *ortho*-C-H borylation of anilines (**12**, Scheme 6) [70]. The methodology employed HBpin as a boron source, $[Ir(OMe)(COD)]_2$ as a precatalyst, and 3,4,7,8-tetramethyl-1,10-phenanthroline (tmphen) as a ligand (Scheme 6).

The C-H borylation reaction was found to be more effective when using tmphen as a ligand and HBpin as a boron source. Various electronically different and differently monosubstituted anilines were borylated at the *ortho* position. For instance, electron-rich 4-methoxyaniline gave the corresponding *ortho*-borylated product **13c** in 63% yield. Electron-

deficient anilines such as 4-trifluoromethyl and 4-cyanoanilines afforded the corresponding borylation products **13b** and **13d** in decent yields of 87%, and 60%, respectively (Scheme 6).

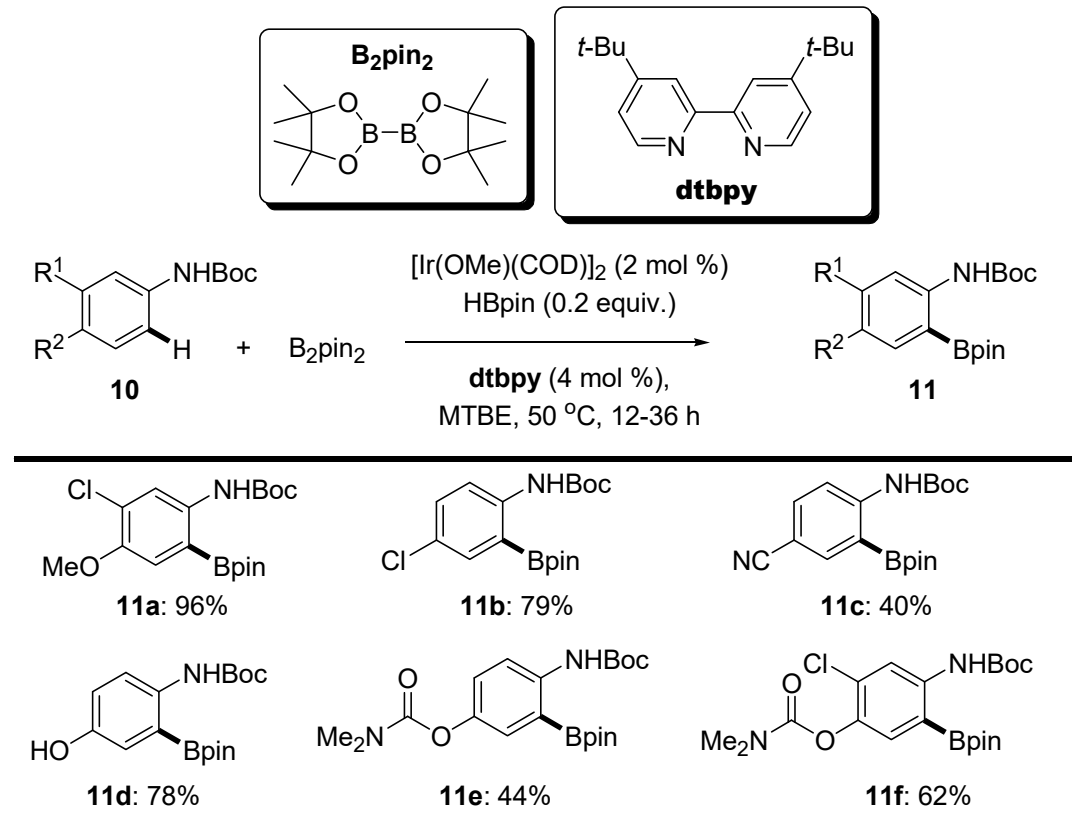

Scheme 5. NH-Boc directed Ir-Catalyzed C-H *ortho*-borylation of protected anilines.

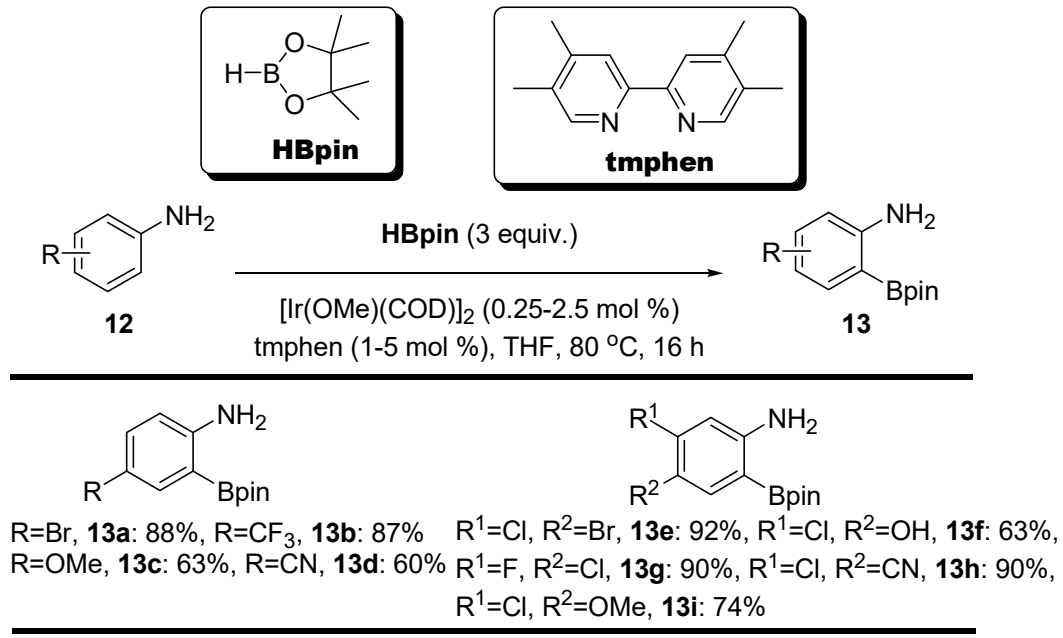

Scheme 6. Ir-catalyzed C-H *ortho*-borylation of anilines.

3,4-Disubstituted anilines also participated in the Ir-catalyzed *ortho*-C-H borylation. For example, electron-rich 3-chloro-4-hydroxyaniline and 3-chloro-4-methoxyanilines gave

the corresponding *ortho*-borylated anilines **13f** and **13i** with yields of 63% and 74%, respectively. Other disubstituted anilines such as dihalogenated 3-chloro-4-bromoaniline and the electron-poor 3-chloro-4-cyanoanilines gave the corresponding *ortho*-borylated anilines **13e** and **13h** in 92% and 90%, yields respectively (Scheme 6).

The regioselectivity of the borylation reaction was rationalized by hydrogen bonding between H in *N*-Bpin aniline and *O* in the Ir complex **14B** in the postulated transition state shown (Figure 4). Principally, this is similar with previous mechanistic findings of the Ir-catalyzed *ortho* C-H borylation reported earlier (Scheme 5) where hydrogen bonding associates Bpin and NH Boc moieties to produce transition state **14A** (Figure 4). It is noteworthy that unsubstituted anilines were not effective under the reaction conditions. Detailed mechanisms of Ir-catalyzed C-H borylation and directed Ir-catalyzed C-H borylation are given and discussed in Schemes 2 and 4 (*vide supra*).

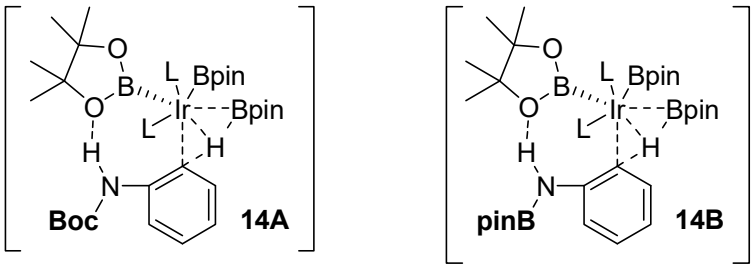

Figure 4. Hydrogen bonding between N-Bpin-aniline and O in the Bpin moiety.

The reaction mechanism was investigated and thus formulated (Scheme 7). Aniline **10** undergoes *N* borylation to give *N*-Bpin aniline **10A**. The N-borylated intermediate then undergoes Ir-catalyzed *ortho* C-H borylation to give bis-borylated aniline **10B**. Work up affords the *ortho*-borylated aniline **11** (Scheme 7).

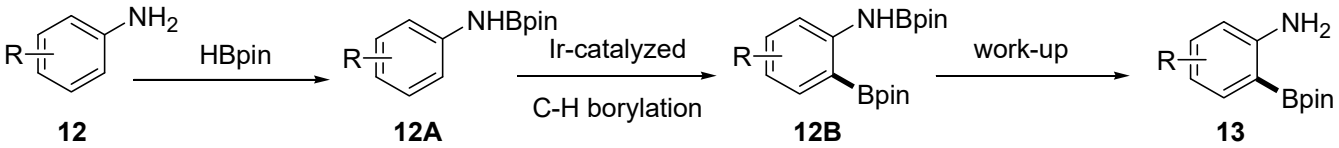

Scheme 7. Mechanism for Ir-catalyzed C-H borylation of anilines.

It was observed that the *ortho*-selectivity of the reaction was greatly reduced when B_2Pin_2 was used instead of HBpin as a borylating agent. When B_2Pin_2 is used, aniline is not borylated at *N*. As a result, this suggests that NHBpin is a better directing group than NH_2 in the Ir-catalyzed C-H borylation. Interestingly, when secondary anilines are used instead of anilines, the *ortho* selectivity is not observed. For example, when *N*-methyl-3-chloroaniline (**15**, Scheme 8) is subjected to the reaction conditions, *ortho*-borylated aniline is not produced. Instead, *meta*-related product **16** is formed in 86% yield (Scheme 8).

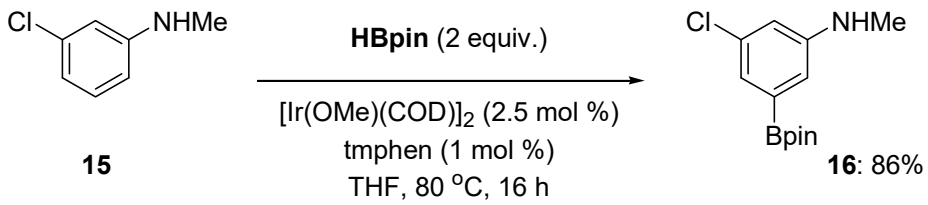

Scheme 8. Ir-catalyzed C-H borylation of N-methyl aniline.

2.2. Amides

In 2019, the Ir-catalyzed *ortho*-C-H borylation of secondary aromatic amides was reported (**17**, Scheme 9) [71]. The borylation occurs with high *ortho*-selectivity and is

governed by hydrogen-bonding interactions. The directed Ir-catalyzed C-H borylation employed $[Ir(OMe)(COD)]_2$ as a precatalyst and B_2pin_2 as a boron source, and a bipyridine-based ligand that has an indole amide (BAIPy) was used (Scheme 7). Investigations of the borylation reaction were performed on various secondary amides using BAIPy ligand and 2,2′-bipyridine (Bpy) itself in control experiments. Exceptionally high *ortho*-selectivity was obtained using the BAIP ligand, whereas no such selectivity was observed using the Bpy ligand. For example, *N*-methylbenzamide gave the corresponding *ortho*-borylated product **18a** in 94% yield. Electron-rich 3-methyl *N*-methyl benzamide gave the corresponding ortho-borylated product **18b** in a 94% yield. *para*-Substituted *N*-methyl benzamides were successfully borylated to produce the corresponding *ortho*-borylated products with exceptionally high yields. For instance, electron-rich 4-Me (**18c**), 4-OMe (**18d**), and 4-*t*-Bu (**16f**) *ortho*-borylated products were obtained in 97%, 92%, and 76% yields, respectively. Electron-deficient 4-CF_3 (**18e**), 4-Ph (**18f**), and 4-Cl (**18h**) *ortho*-borylated products were obtained in 99%, 90%, and 91% yields, respectively (Scheme 9).

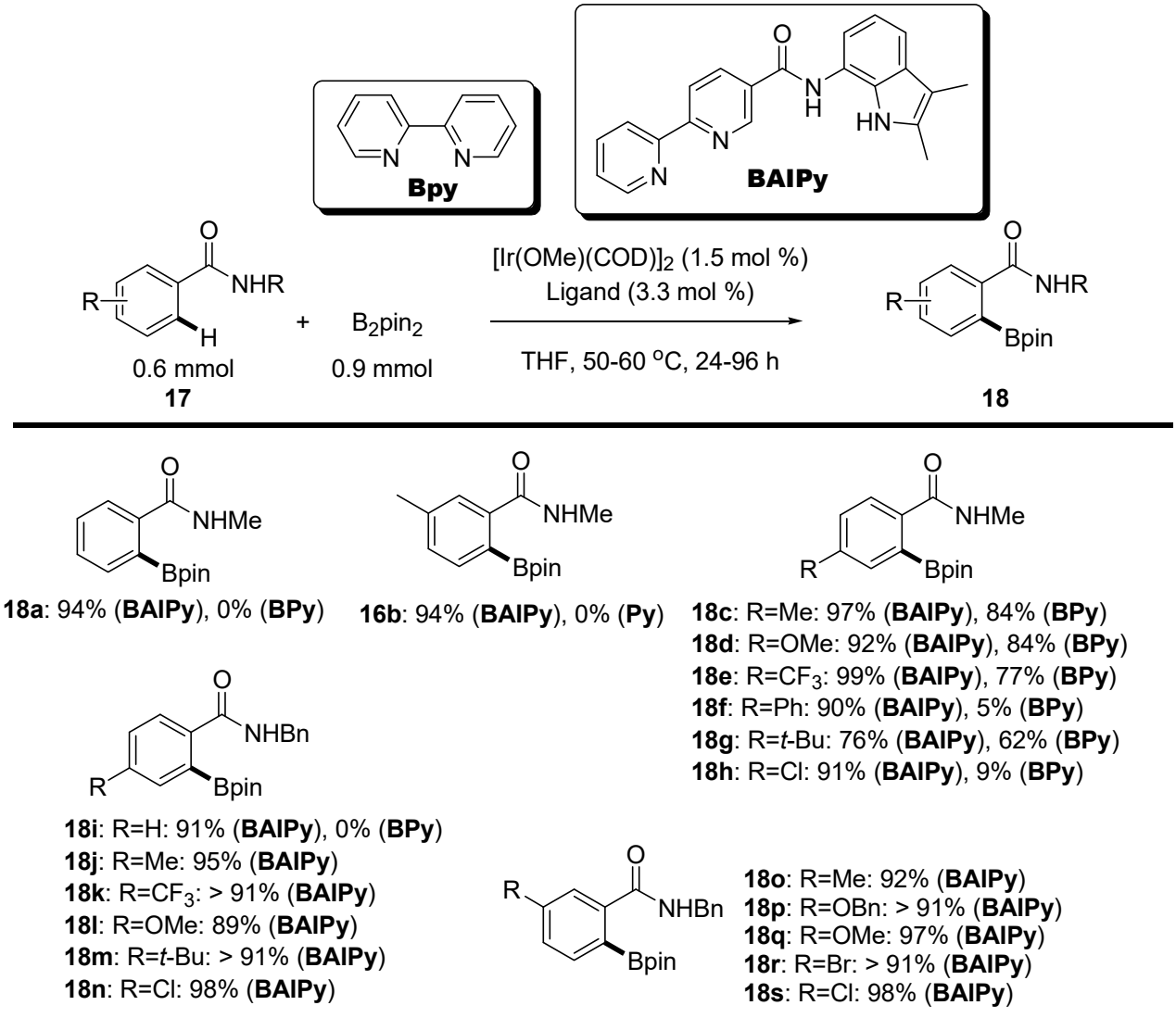

Scheme 9. Ir-BAIPy-based directed C-H borylation of secondary amides.

ortho-Borylated products of 4-substituted N-benzylbenzamides were also obtained in high yields. For example, electron-rich 4-Me (**18j**), 4-OMe (**18l**), and 4-*t*-Bu (**18m**) *ortho*-borylated products were obtained in 95%, 89%, and >91% yields, respectively. Electron-deficient 4-CF_3 (**18k**) and 4-Cl (**18n**) *ortho*-borylated products were obtained in >91% and

98% yields, respectively (Scheme 9). Electron-donating and electron-withdrawing groups are equally tolerated and delivered *ortho*-borylated products with excellent yields.

ortho-Borylated products of 3-substituted *N*-benzylbenzamides were also obtained with remarkably high yields. For example, electron-rich 3-Me (**18o**), 3-OMe (**18q**), and 3-OBn (**18p**) *ortho*-borylated products were obtained in 92%, 97%, and >91% yields, respectively. Halogenated products, such as 3-Br (**18r**), and 3-Cl (**18s**) *ortho*-borylated products were obtained in >91% and 98% yields, respectively (Scheme 9). This is a demonstration of halogen tolerance in the reaction.

It was postulated that the benzamide substrate reorganizes itself to interact with the indole and the amide moieties in the BAIPy ligand by hydrogen bonding to form a hydrogen-bonding-based transition state **19** (Figure 5). This prerequisite hydrogen bonding brings the Ir-metal center in proximity to the *ortho*-C-H bond, setting the stage for C-H bond cleavage followed by subsequent borylation with Bpin.

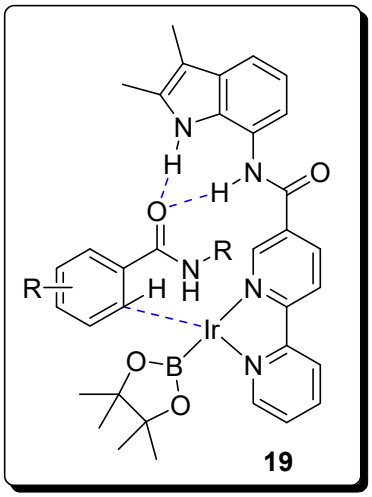

Figure 5. Hydrogen-bonding transition state for the directed C-HJ borylation.

In 2021, tertiary benzamides have been reported to undergo Ir-catalyzed *ortho*-C-H borylation that employs $[Ir(OMe)(COD)]_2$ as a precatalyst and B_2pin_2 as a boron source [72]. The borylation reaction features a unique 3-thiophenylpyridine ligand (**20**, Scheme 10). Bipyridine ligands did not take part in the *ortho*-selective C-H borylation. However, 2-phenylpyridines were found to be effective in the reaction, which led to the development of the 3-thiophenylpyridine ligand. It was postulated that the reactivity of this ligand was attributed to the higher acidity of the thiophenyl group at C2. Consequently, upon reaction with $[Ir(OMe)(COD)]_2$, the ligand forms a cyclometalated complex with Ir, which sets the stage for C-H borylation.

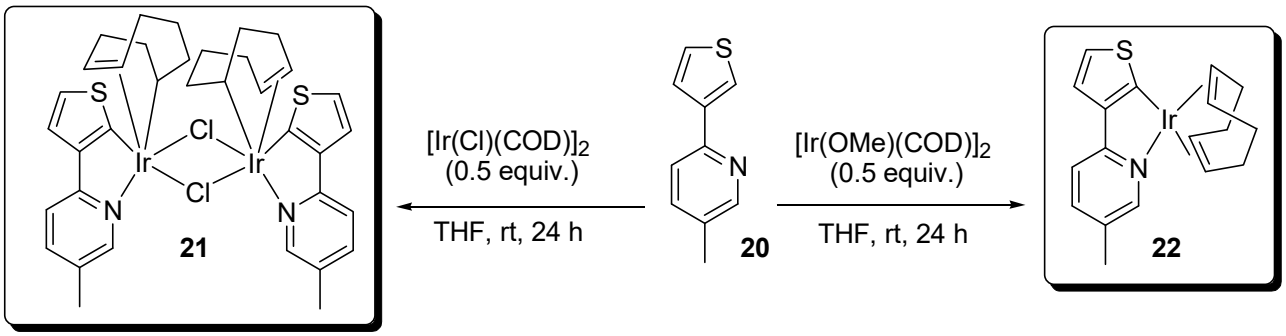

Scheme 10. Formation of cyclometallated.

To investigate the active catalyst system, ligand **20** was treated with two Ir precatalysts: $(Ir(Cl)(COD)]_2$ and $[Ir(OMe)(Cod)]_2$ (Scheme 10).

When the 3-thiophenylpyridine ligand was treated with the former, a cyclometallated dimeric iridium(III) complex **21** was formed. This complex was presumably formed by metal-mediated hydride transfer. When the ligand was treated with the latter, the Ir(I)-cyclometallated complex **22** was formed (Scheme 10). Both cyclometallated complexes were characterized and confirmed by X-ray [72].

After establishing the active catalytic species in the reaction, the scope of the Ir-catalyzed *ortho*-C-H borylation of tertiary benzamides (**23**, Scheme 11) was carried out under developed reaction conditions. The effects of substituents on *N* were studied under the reported optimum conditions (Scheme 11). Thus, various alkyl groups were compatible with the reaction conditions and were able to promote Ir-catalyzed *ortho*-selective C-H borylation of their benzamides. For example, *ortho*-borylated *N*,*N*-dicyclohexylbenzamide (**24a**) was obtained in 94% yield. The *N*,*N*-dimethyl counterpart (**24b**) was obtained in 82% yield, and *N*,*N*-diethyl (**24c**) and N,N-dihexyl (**24d**) benzamides were obtained in 92% yields. Other *ortho*-borylated benzamides of pyrrolidinyl (**24i**) and morphine (**24j**) groups were obtained in yields of 88% and 86%, respectively (Scheme 11).

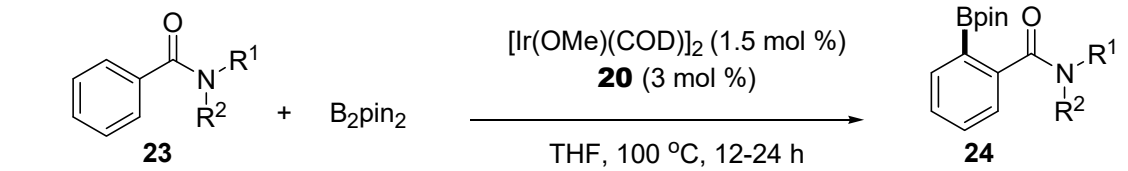

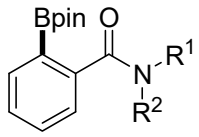

24a: R^1=R^2=Cyhex: 94%
24b: R^1=R^2=Me: 82%
24c: R^1=R^2=Et: 92%
24d: R^1=R^2=*n*-Hex: 92%

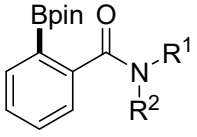

24e: R^1=*i*-Pr, R^2=Me: 90%
24f: R^1=*n*-Hex, R^2=Me: 86%
24g: R^1=*t*-Bu, R^2=Me: 93%
24h: R^1=Cychex, R^2=Me: 90%

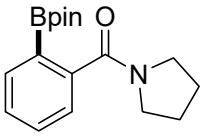

24i: 88%

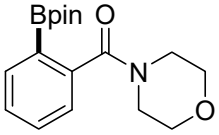

24j:86%

Scheme 11. Effects of *N*-substituents of Ir-catalyzed C-H borylation of tertiary benzamides.

The scope of the arene unit was explored using its *N*,*N*-diisopropylbenzamides (**25**, Scheme 12). Here, 2-substituted *N*,*N*-diisopropylbenzamides were successfully borylated at the *ortho* position to give the corresponding electron-rich 2-methyl (**26a**) and 2-phenyl (**26b**) benzamides in 82% and 73% yields, respectively. Various 3-substituted *N*,*N*-diisopropyl benzamides were tested under optimum reaction conditions. For example, *ortho*-borylated electron-rich 3-OMe (**26c**), 3-O*n*-Bu (**26h**), 3-Me (**26e**), and 3-Ph (**26f**) benzamides were obtained in 92%, 93%, 95%, and 93% yields, respectively. A bromo substituent was tolerated to give the corresponding *ortho*-borylated product (**26d**) in 86% yield. Electron-withdrawing groups such as CF_3 were also tolerated, giving rise to the corresponding *ortho*-borylated product (**26g**) in 90% yield (Scheme 12) [72].

In addition, the scope of *para*-substitution was explored using *N*,*N*-diisopropylbenzamides (Scheme 12). For example, *ortho*-borylated electron-rich 3-Me (**26i**), 3-OMe (**26j**), 3-O*n*-Bu (**26n**), and 3-Ph (**26l**) benzamides were obtained in 98%, 92%, 96%, and 98% yields, respectively. A bromo substituent was tolerated to give the corresponding *ortho*-borylated product (**26k**) in a 94% yield. Electron-withdrawing groups such as CF_3 were also tolerated, giving rise to the corresponding *ortho*-borylated product (**26m**) in 86% yield (Scheme 12). The reaction tolerates differently substituted and electronically different benzamides.

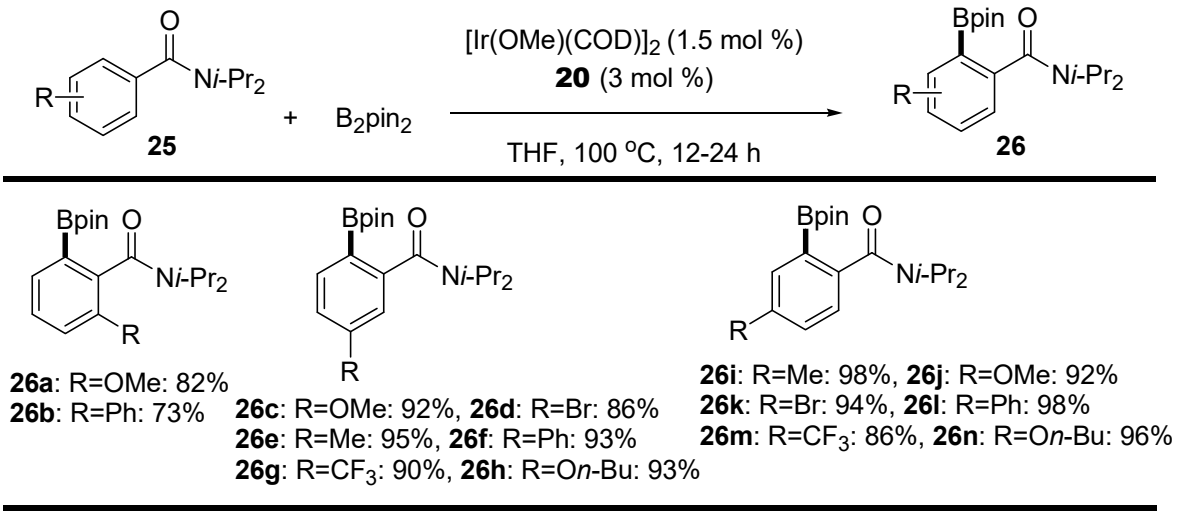

Scheme 12. Arene scope of Ir-catalyzed C-H borylation of tertiary benzamides.

The versatility of the developed Ir-catalyzed *ortho*-C-H borylation with the thiophenylpyridine ligand was demonstrated by tolerance of various functional groups (**27**, Scheme 13) [72]. Thus, a functional group scope was explored under optimum reaction conditions (Scheme 12). For example, ketone, esters, and carbamates tolerated the reaction conditions to give the corresponding *ortho*-borylated arene products (**28a**), (**28b**), (**28d**), (**25e**), and (**28f**) in 91%, 69%, 80%, 71%, and 91% yields, respectively. Other *N*-based directing groups such as an imine, aniline, and benzylamine were also tolerated to give the corresponding *ortho*-borylated arene products (**28c**), (**28g**), and (**28j**) in 86%, 73%, and 93% yields, respectively. Methylthio and OMOM directing groups were tolerated as well, giving rise to the corresponding *ortho*-borylated arene products (**28h**) and (**28i**) in 82% and 68% yields, respectively (Scheme 13) [72].

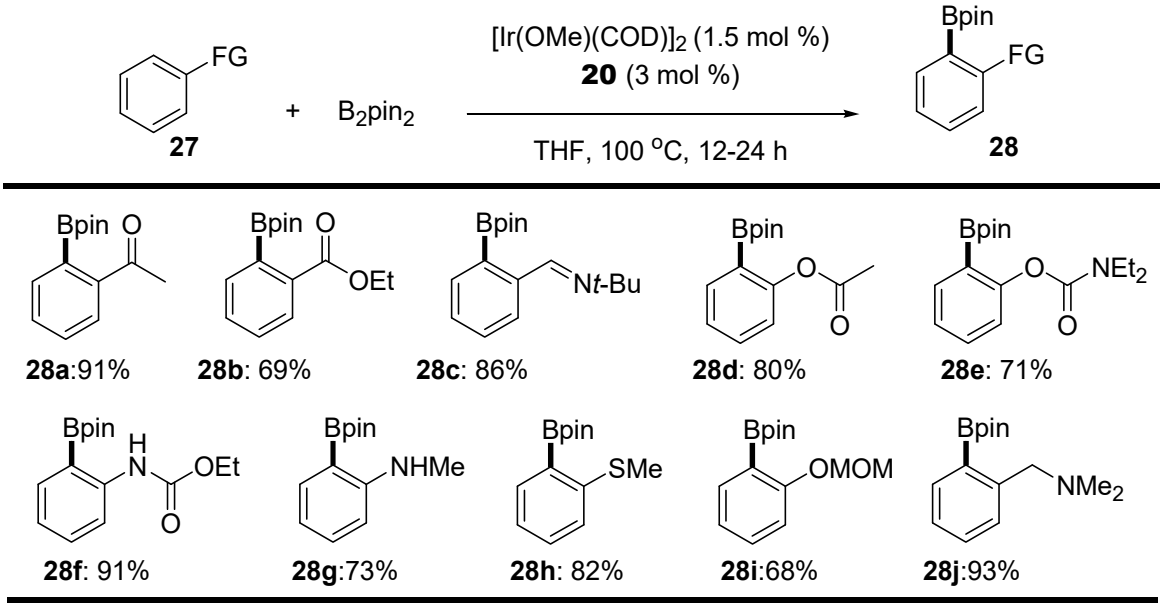

Scheme 13. Functional group scope of Ir-catalyzed C-H borylation using thiophenylpyridine as a ligand.

In 2023, another *ortho*-selective borylation method for tertiary amides (**29**, Scheme 14) was reported [73]. The borylation was Ir catalyzed employing $[Ir(OMe)(COD)]^2$ as a precatalyst and B_2pin_2 as a boron source, and 5-CF_3 substituted bipyridine ligand CF_3-Bpy was

used (Scheme 14). The Ir-catalyzed C-H borylation delivered *ortho*-borylated benzamides in good yields. Tertiary benzamides with different *N*-substituents were successfully borylated at the *ortho* position to give the corresponding *N*,*N*-dimethyl, *N*,*N*-dicyclohexyl, *N*,*N*-diphenyl, and *N*-methyl-*N*-methoxy *ortho*-borylated arene products (**30a**), (**30b**), (**30c**), and (**30d**) in 83%, 98%, 85%, and 83% yields, respectively. Secondary benzamides were also tolerated under optimum reaction conditions to give the corresponding *N*-methyl, *N*-Ph, and *N*-C_6F_5 *ortho*-borylated arene products (**30e**), (**30f**), and (**30g**) in 87%, 83%, and 41% yields, respectively. Ester and ketone functional groups delivered the corresponding *ortho*-borylated arene products (**30h**) and (**30i**) in yields of 64% and 81%, respectively. Other functional groups that are based on indole, sulfoxide, and ester-functionalized amide gave the corresponding *ortho*-borylated arene products (**30j**), (**30k**), and (**30l**) in 73%, 99%, and 57% yields, respectively (Scheme 14).

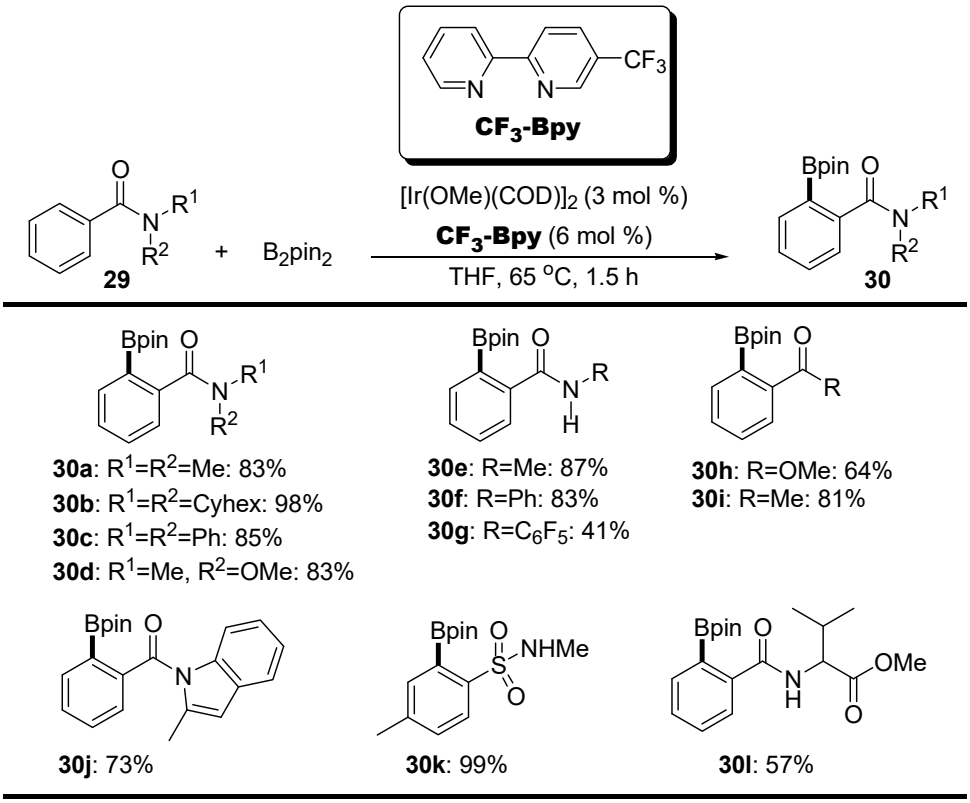

Scheme 14. Ir-catalyzed C-H borylation using 5-CF_3-bipyridine ligand.

2.3. Benzyl Amines

In 2012, Ir-catalyzed *ortho*-selective C-H borylation of benzylic amines (**31**, Scheme 15) was developed [74]. The reaction employs $[Ir(OMe)(COD)]_2$ as a precatalyst, B_2pin_2 as a boron source, and features picolyl amine as a ligand.

Differently substituted *N*,*N*-dimethylbenzylamines were successfully borylated at the *ortho* position using the developed borylation methodology (Scheme 15). For example unsubstituted *N*,*N*-dimethylbenzylamine, electron-rich 2-methyl-*N*,*N*-dimethylbenzylamine and electron-poor 2-fluoro-N,N-dimethylbenzylamine were borylated at *ortho* positions to give the corresponding *ortho*-borylated products (**32a**), (**32b**), and (**32c**) in 63%, 73%, and 74% yields, respectively. *meta*-Substituted *N*,*N*-dimethylbenzylamines such as electron-rich 3-Me, 3-OMe, and 3-Cl gave the corresponding *ortho*-borylated products (**32d**), (**32e**), and (**32f**) in 55%, 82%, and 54% yields, respectively. *para*-Substituted *N*,*N*-dimethylbenzylamines such as 4-Me, 4-CO_2Et, and 4-Br gave the corresponding *ortho*-borylated products (**32g**), (**32h**), and (**32i**) in 81%, 49%, and 37% yields, respectively (Scheme 15) [74].

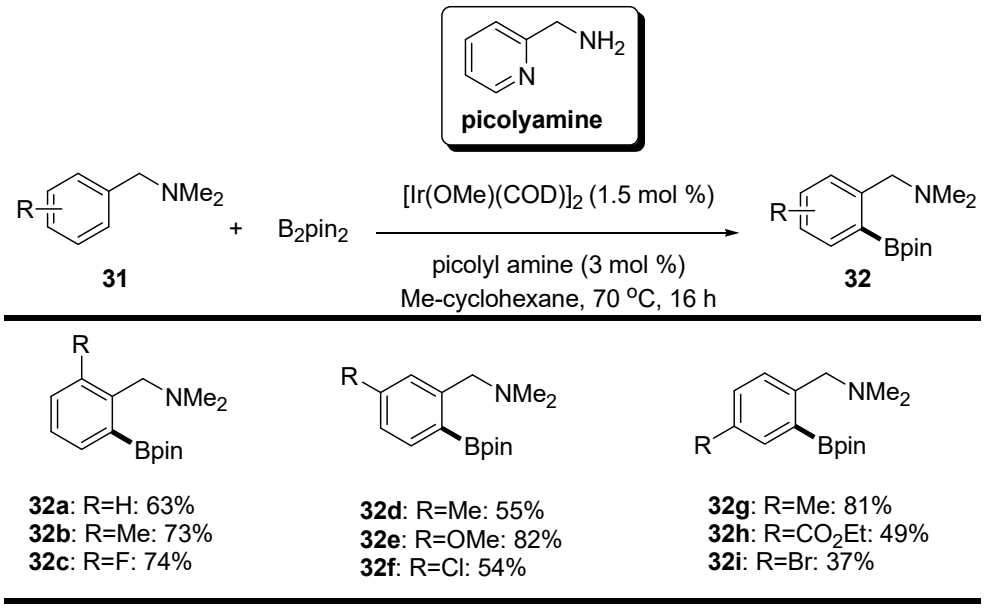

Scheme 15. Ir-catalyzed C-H borylation of benzylamines.

A key structural feature of picolyamine is that it possesses an N-H bond that could form an H-bond with a benzylamine substrate. Thus, a transition Ir-complex was proposed, where picolyamine binds to the Ir precatalyst, forms hydrogen bonding with the benzylamine substrate, and makes a vacant coordination site on the Ir center available (**34**, Figure 6). Consequently, *ortho*-C-H cleavage followed by borylation of the benzylamine subsequently occur. Detailed mechanisms of Ir-catalyzed C-H borylation and directed Ir-catalyzed C-H borylation are given and discussed in Schemes 2 and 4 (*vide supra*).

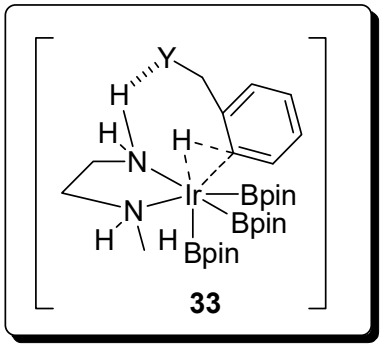

Figure 6. Proposed transition state for the Ir-catalyzed C-H borylation of benzylamines.

A scope of amine directing effect was explored under optimum reaction conditions of the picolylamine-promoted Ir-catalyzed *ortho*-C-H borylation (Scheme 16). For example, *N*,*N*-dimethyl-2-phenylethylamine was borylated at the arene *ortho* position to give the corresponding *ortho*-borylated product **35a** in a moderate 51% yield. A more sterically hindered benzylamine such as *N*,*N*-dimethyl-1-phenylethylamine gave corresponding *ortho*-borylated product **35b** in 86% yield. Imidazolidine-based benzylamine was successfully borylated at the arene *ortho* position to give the corresponding *ortho*-borylated product **35c** in a moderate 71% yield (Scheme 16) [74].

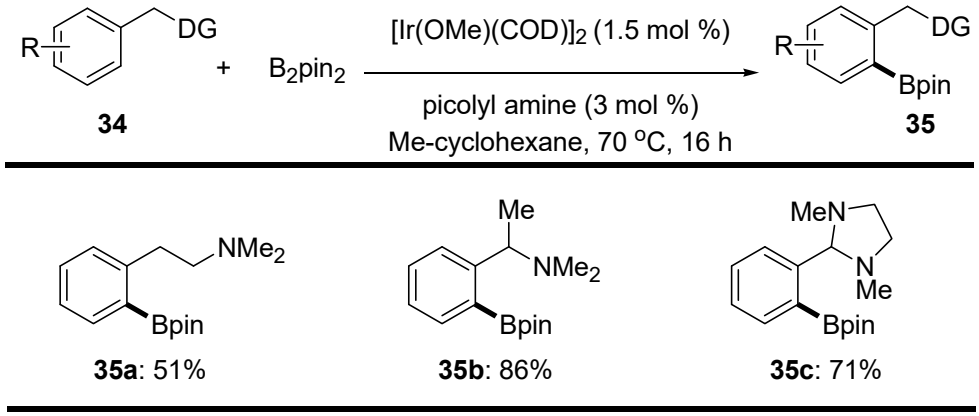

Scheme 16. Amine directing effect scope of Ir-catalyzed C-H borylation of benzylamines.

In 2019, an asymmetric enantioselective Ir-catalyzed aromatic *ortho*-C-H borylation of diaryl *N*,*N*-dimethyamines was reported [75]. The reaction employs $[Ir(Cl)(COD)]_2$ as a precatalyst and B_2pin_2 as a boron source. The key feature of the regioselective asymmetric reaction is the use of chiral (S,S)-DPEN-derived bidentate boryl ligands, and the reaction features picolyl amine as a ligand.

The enantioselectivity in the asymmetric Ir-catalyzed C-H borylation relied on the use of chiral boryl silyl ligand (**36**, Scheme 17) that is based on commercially available (*S*,*S*)-DPEN. It was proposed that upon treatment of such chiral ligands with [Ir]-B_2pin_2, a vacant coordination site on the Ir center gives the proposed active catalytic Ir species **37** (Scheme 17).

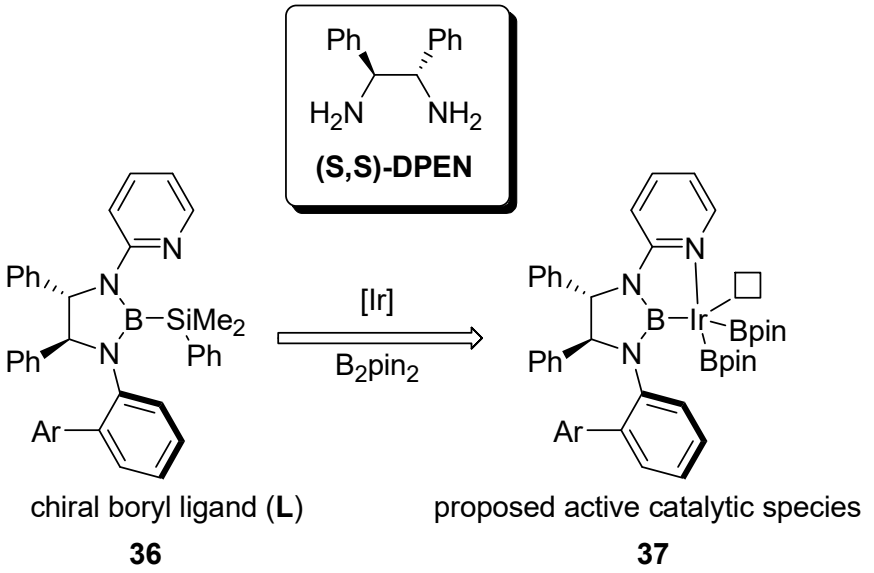

Scheme 17. Use of chiral DPEN-derived boryl ligand and the proposed active Ir catalyst.

The chiral ligand where the aryl group is 3,5-dimethylphenyl was found to be the optimum ligand. A wide range of diphenyl *N*,*N*-dimethyl amines (**38**, Scheme 18) was successfully borylated in a regioselective and enantioselective manner (Scheme 18). For example, chiral borylated product **39a** was obtained in 88% yield and an excellent enantioselectivity of 94% ee. Other substituted amines on the aryl groups such as electron-rich 4-Me and 4-OMe and electron-poor 4-CF_3 and 4-OCF_3 were borylated at the *ortho* position with good yields and enantioselectivities to give *ortho* borylated products **39b**, **39c**, **39d**, and **39e** in 70%, 76%, 65%, and 86% yields and enantioselectivities of 88% ee, 85% ee, 95% ee, and 82% ee, respectively. Differently substituted *ortho*-borylated products such as **39f**, **39g**, **39h**,

and **39i** were also obtained in 65%, 70%, 61%, and 89% yields and enantioselectivities of 92% ee, 87% ee, 82% ee, and 91% ee, respectively (Scheme 18) [75].

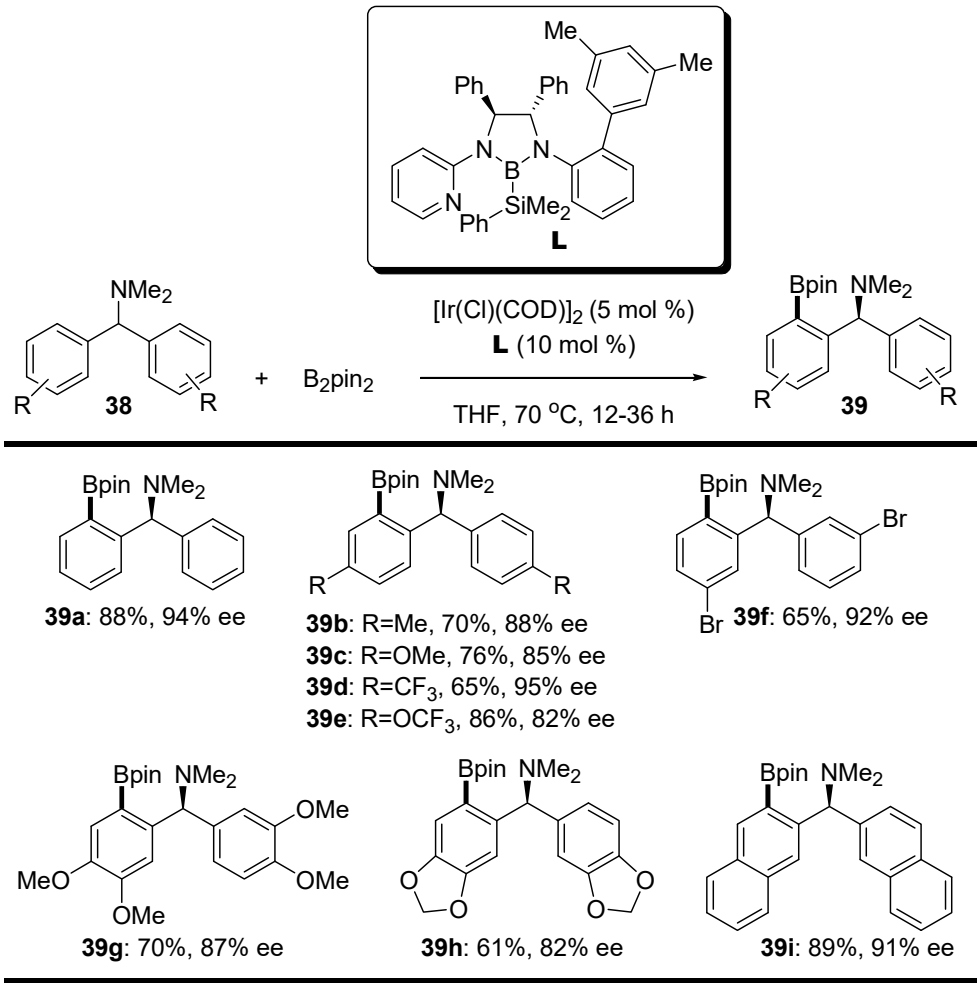

Scheme 18. Ir-catalyzed regioselective asymmetric C-H borylation.

2.4. Hydrazones

In 2012, Ir-catalyzed *ortho*, *ortho*′-C-H diborylation of aromatic *N*,*N*-dimethylhydrazones (**40**, Scheme 19) was reported [76]. The reaction employs $[Ir(OMe)(COD)]_2$ as a pre-catalyst, and B_2pin_2 as a boron source with a catalytic amount of HBpin. The developed diborylation reaction features the use of hemilabile pyridine-hydrazone *N*,*N*-ligand (**L**, Scheme 19).

The reaction tolerated a good range of substituted aryl hydrazones (Scheme 18). While unsubstituted substrate delivered the diborylation product **41a** in 76% yield, the 3-Cl and electron-rich 3-OMe counterparts gave the corresponding o,o′-diborylated hydrazones **41b** and **41c** in 72% and 58% yields, respectively. In addition, other substituted aryl hydrazones such as 4F, 3,4-dichloro, and 3,5-dimethoxy were successfully diborylated to give the corresponding o,o′-diborylated hydrazones **41d**, **41e**, and **41f** in 79%, 51%, and 60% yields, respectively (Scheme 19) [76].

The obtained o,o′-diborylated hydrazones were then further functionalized using the Suzuki–Miyaura cross-coupling reaction to provide access to the desired coupled products. The developed Ir-catalyzed selective o,o′-diborylation methodology provided access to densely functionalized benzaldehyde derivatives.

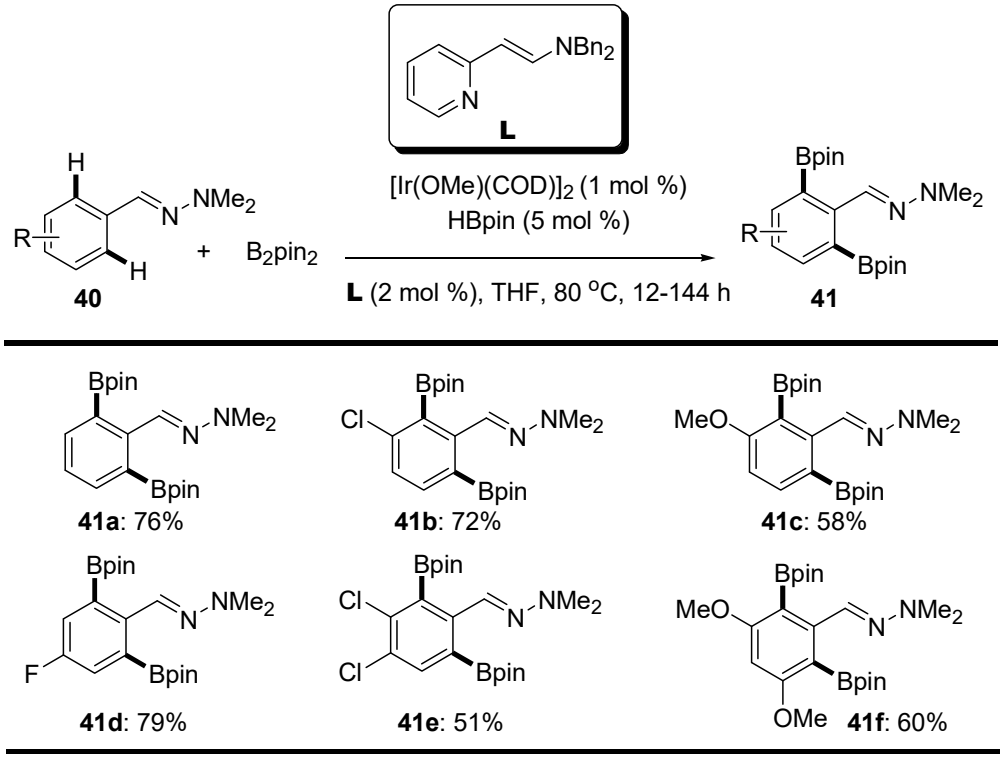

Scheme 19. Ir-catalyzed C-H borylation of aryl hydrazones based on pyridine-hydrazone ligand.

2.5. Triazines

In 2022, aryl triazines (**42**, Scheme 20) were reported to undergo ligand-free Ir-catalyzed C-H *ortho-ortho'*-diborylation [77]. The C-H borylation was directed by the triazine and employed $[Ir(OMe)(COD)]_2$ as a precatalyst and B_2pin_2 as a boron source. The triazine functioned as both substrate and ligand; thus, no external ligand was necessary.

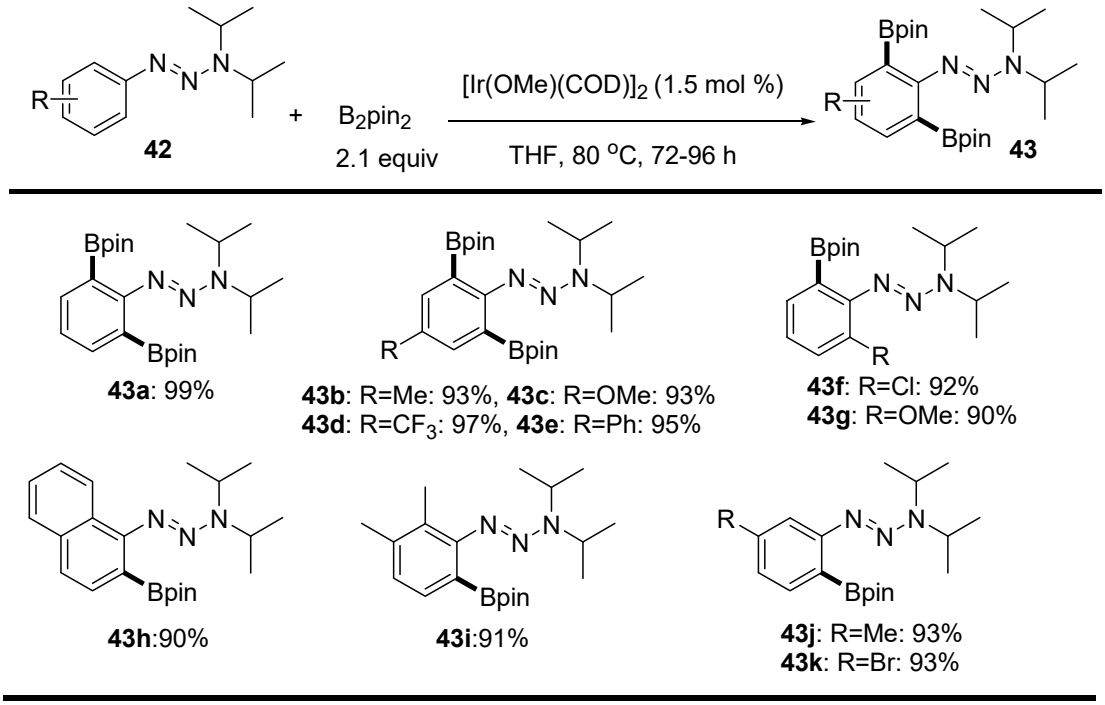

Scheme 20. Ligand-free Ir-catalyzed C-H borylation of aryl triazines.

N,*N*-Diisopropyl aryl triazine was found to be the most effective under optimum reaction conditions (Scheme 20). Thus, unsubstituted *N*,*N*-diisopropyl aryl triazine was diborylated at both *ortho* positions to give bisborylated product **43a** in a remarkable 99% yield. *para*-Substituted aryl *N*,*N*-diisopropyltriazines were successfully diborylated as well. Other *ortho*-*ortho*′-diborylated electron-rich 4-Me (**43b**) and electron-poor 4-OMe (**43c**), 4-CF_3 (**43d**), and 4-Ph (**43e**) borylated products were obtained in 93%, 93%, 97%, and 95% yields, respectively. *ortho*-Substituted aryl *N*,*N*-diisopropyltriazines such as 2-Cl and 2-OMe were also borylated at the *ortho*-position to give the corresponding *ortho*-borylated products 2-Cl (**43b**) and 2-OMe (**43c**) in 92% and 90% yields. Other differently substituted aryl triazines as evidenced by **43h** and **43i** which were obtained in 90% and 91% yields. *meta*-Substituted aryl *N*,*N*-diisopropyltriazines such as 3-Me and 3-Br were also successfully borylated at the respective *ortho* position to give the corresponding *ortho*-borylated products **36j** and **36k** in 93% yields (Scheme 19). The reaction scope performed showed good functional group tolerance (Scheme 20) [77].

3. Conclusions

Directed Ir-catalyzed C-H borylation is a significant type of C-H bond functionalization. The directed borylation provides borylated products in a regioselective manner. Specifically, *ortho*-regioselective Ir-catalyzed C-H borylation of arenes directed by N-containing directing groups is of unique importance. Various *N*-bearing directing groups have been proven to be effective in steering Ir-catalyzed C-H borylation to occur at *ortho* positions in a regioselective manner. The directed C-H borylation was demonstrated by various N-bearing directing groups, including anilines, amides, benzyl amines, hydrazones, and triazines. The directing ability of such directing groups lies in their coordination power with vacant sites on intermediate Ir-catalytic species, thus setting the stage for interactions between the Ir center and an *ortho* C-H bond and facilitating C-H borylation through C-H bond cleavage.

Funding: This research received no external funding.

Conflicts of Interest: The author declares no conflict of interest.

References

1. Shilov, A.E.; Shul'pin, G.B. Activation of C–H Bonds by Metal Complexes. *Chem. Rev.* **1997**, *97*, 2879–2932. [CrossRef]
2. Kakiuchi, F.; Chatani, N. Catalytic Methods for C–H Bond Functionalization: Application in Organic Synthesis. *Adv. Synth. Catal.* **2003**, *345*, 1077–1101. [CrossRef]
3. Engle, K.M.; Mei, T.-S.; Wasa, M.; Yu, J.Q. Weak Coordination as a Powerful Means for Developing Broadly Useful C–H Functionalization Reactions. *Acc. Chem. Res.* **2012**, *45*, 788–802. [CrossRef]
4. Rej, S.; Das, A.; Chatani, N. Strategic Evolution in Transition Metal-Catalyzed Directed C–H Bond Activation and Future Directions. *Coord. Chem. Rev.* **2021**, *431*, 213683–213719. [CrossRef]
5. Al Mamari, H.H.; Štefane, B.; Žugelj, H.B. Metal-Catalyzed C–H Bond Functionalization of Phenol Derivatives. *Tetrahedron* **2020**, *76*, 130925–130936. [CrossRef]
6. Docherty, J.H.; Lister, T.M.; Mcarthur, G.; Findlay, M.T.; Domingo-Legarda, P.; Jacob Kenyon, J.; Choudhary, S.; Igor Larrosa, I. Transition-Metal-Catalyzed C–H Bond Activation for the Formation of C–C Bonds in Complex Molecules. *Chem. Rev.* **2023**, *123*, 7692–7760. [CrossRef]
7. Dalton, T.; Faber, T.; Glorius, F. C–H Activation: Toward Sustainability and Applications. *ACS Cent. Sci.* **2021**, *2*, 245–261. [CrossRef]
8. He, J.; Wasa, M.; Chan, K.S.L.; Shao, Q.; Yu, J.-Q. Palladium-Catalyzed Transformations of Alkyl C–H Bonds. *Chem. Rev.* **2017**, *117*, 8754–8786. [CrossRef]
9. Chen, X.; Engle, K.M.; Wang, D.-H.; Yu, J.-Q. Palladium(II)-Catalyzed C–H Activation/C-C Cross-Coupling Reactions: Versatility and Practicality. *Angew. Chem. Int. Ed.* **2009**, *48*, 5094–5115. [CrossRef]
10. Neufeldt, S.R.; Sanford, M.S. Controlling Site Selectivity in Palladium-Catalyzed C–H Bond Functionalization. *Acc. Chem. Res.* **2012**, *45*, 936–946. [CrossRef]
11. Bay, K.L.; Yang, Y.-F.; Houk, K.N. Multiple Roles of Silver Salts in Palladium-Catalyzed C–H Activations. *J. Organomet. Chem.* **2018**, *864*, 19–25. [CrossRef]
12. Colby, D.A.; Tsai, A.S.; Bergman, R.G.; Ellman, J.A. Rhodium Catalyzed Chelation-Assisted C–H Bond Functionalization Reactions. *Acc. Chem. Res.* **2012**, *45*, 814–825. [CrossRef]

13. Rej, S.; Chatani, N. Rhodium-Catalyzed C(sp^2)- or C(sp^3)–H Bond Functionalization Assisted by Removable Directing Groups. *Angew. Chem. Int. Ed.* **2019**, *58*, 8304–8329. [CrossRef]
14. Lewis, J.C.; Bergman, R.G.; Ellman, J.A. Direct Functionalization of Nitrogen Heterocycles via Rh-Catalyzed C–H Bond Activation. *Acc. Chem. Res.* **2008**, *41*, 1013–1025. [CrossRef]
15. Vasquez-Cespedes, S.; Wang, X.; Glorius, F. Plausible Rh(V) Intermediates in Catalytic C–H Activation Reactions. *ACS Catal.* **2018**, *8*, 242–257. [CrossRef]
16. Song, G.; Li, X. Substrate Activation Strategies in Rhodium(III)-Catalyzed Selective Functionalization of Arenes. *Acc. Chem. Res.* **2015**, *48*, 1007–1020. [CrossRef]
17. Singh, K.S. Recent Advances in C–H Bond Functionalization with Ruthenium-Based Catalysts. *Catalysts* **2019**, *9*, 173/1–173/51. [CrossRef]
18. Dana, S.; Yadav, M.R.; Sahon, A.K. Ruthenium-Catalyzed C-N and C–O Bond-Forming Processes from C–H Bond Functionalization. *Top. Organomet. Chem.* **2016**, *55*, 189–215.
19. Ruiz, S.; Villuendas, P.; Urriolabeitia, E.P. Ru-catalyzed C-H functionalizations as a tool for selective organic synthesis. *Tetrahedron Lett.* **2016**, *57*, 3413–3432. [CrossRef]
20. Li, B.; Dixneuf, P.H. Ruthenium(II)-Catalyzed sp^2 C–H Bond Functionalization by C–C Bond Formation. *Top. Organomet. Chem.* **2015**, *48*, 119–193.
21. Ackermann, L.; Vicente, R. Ruthenium-Catalyzed Direct Arylations through C–H Bond Cleavages. *Top. Curr. Chem.* **2010**, *292*, 211–229.
22. Gandeepan, P.; Müller, T.; Zell, D.; Warratz, S.; Ackermann, L. 3d Transition Metals for C–H Activation. *Chem. Rev.* **2019**, *119*, 2192–2452. [CrossRef]
23. Khake, S.M.; Chatani, N. Chelation-Assisted Nickel-Catalyzed C–H Functionalizations. *Trends Chem.* **2019**, *1*, 524–539. [CrossRef]
24. Khake, S.M.; Chatani, N. Nickel-Catalyzed C–H Functionalization Using A Non-directed Strategy. *Chem* **2020**, *6*, 1056–1081. [CrossRef]
25. Liu, Y.-H.; Xia, Y.-N.; Shi, B.-F. Ni-Catalyzed Chelation-Assisted Direct Functionalization of Inert C-H Bonds. *Chin. J. Chem.* **2020**, *38*, 635–662. [CrossRef]
26. Cano, R.; Mackey, K.; McGlacken, G.P. Recent Advances in Manganese-Catalyzed C-H Activation: Scope and Mechanism. *Catal. Sci. Technol.* **2018**, *8*, 1251–1266. [CrossRef]
27. Liu, W.; Ackermann, L. Manganese-Catalyzed C–H Activation. *ACS Catal.* **2016**, *6*, 3743–3752. [CrossRef]
28. Lanzi, M.; Cera, G. Iron-Catalyzed C-H Functionalizations under Triazole-Assistance. *Molecules* **2020**, *25*, 1806. [CrossRef] [PubMed]
29. Shang, R.; Ilies, L.; Nakamura, E. Iron-Catalyzed C–H Bond Activation. *Chem. Rev.* **2017**, *117*, 9086–9139. [CrossRef] [PubMed]
30. Prakash, S.; Kuppusamy, R.; Cheng, C.H. Cobalt-Catalyzed Annulation Reactions via C–H Bond Activation. *ChemCatChem* **2018**, *10*, 683–705. [CrossRef]
31. Wang, S.; Chen, S.-Y.; Yu, X.-Q. C–H Functionalization by High-Valent Cp*Co(III) Catalysis. *Chem. Commun.* **2017**, *53*, 3165–3180. [CrossRef] [PubMed]
32. Yoshino, T.; Matsunaga, S. High-Valent Cobalt-Catalyzed C–H Bond Functionalization. *Adv. Organomet. Chem.* **2019**, *68*, 197–247. [CrossRef]
33. Baccalini, A.; Vergura, S.; Dolui, P.; Zanoni, G.; Maiti, D. Recent Advances in Cobalt-Catalyzed C-H Functionalizations. *Org. Biomol. Chem.* **2019**, *17*, 10119–10141. [CrossRef] [PubMed]
34. Moselage, M.; Lie, J.; Ackermann, L. Cobalt-Catalyzed C–H Activation. *ACS Catal.* **2016**, *6*, 498–525. [CrossRef]
35. Sambiagio, C.; Schönbauer, D.; Blieck, R.; Dao-Huy, T.; Pototschnio, G.; Schaaf, P.; Wiesinger, T.; Zia, M.F.; Wencel-Delord, J.; Besset, T.; et al. A Comprehensive Overview of Directing Groups Applied in Metal-Catalyzed C–H Functionalization Chemistry. *Chem. Soc. Rev.* **2018**, *47*, 6603–6743. [CrossRef] [PubMed]
36. Omae, I. Intramolecular five-membered ring compounds and their applications. *Coord. Chem. Rev.* **2004**, *248*, 995–1023. [CrossRef]
37. Rouquet, G.; Chatani, N.N. Catalytic Functionalization of C(sp^2)–H and C(sp^3)–H Bonds by Using Bidentate Directing Groups. *Angew. Chem. Int. Ed.* **2013**, *52*, 11726–11743. [CrossRef] [PubMed]
38. Hartwig, J.F. Borylation and Silylation of C–H Bonds: A Platform for Diverse C–H Bond Functionalizations. *Acc. Chem. Res.* **2012**, *45*, 864–873. [CrossRef] [PubMed]
39. Mkhalid, I.A.I.; Barnard, J.H.; Marder, T.B.; Murphy, J.M.; Hartwig, J.F. C–H Activation for the Construction of C–B Bonds. *Chem. Rev.* **2010**, *110*, 890–931. [CrossRef]
40. Neeve, E.C.; Geier, S.J.; Mkhalid, I.A.I.; Westcott, S.; Marder, T.B. Diboron(4) Compounds: From Structural Curiosity to Synthetic Workhorse. *Chem. Rev.* **2016**, *110*, 9091–9161. [CrossRef]
41. Ishiyama, T.; Miyaura, N. Transition metal-catalyzed borylation of alkanes and arenes via C-H activation. *J. Organometal. Chem.* **2003**, *680*, 3–11. [CrossRef]
42. Ishiyama, T.; Takagi, J.; Hartwig, J.F.; Miyaura, N. A Stoichiometric Aromatic C-H Borylation Catalyzed by Iridium(I)/2,2′-Bipyridine Complexes at Room Temperature. *Angew. Chem. Int. Ed.* **2002**, *41*, 3056–3058. [CrossRef]
43. Kuroda, Y.; Nakao, Y. Catalyst-enabled Site-selectivity in the Iridium-catalyzed C–H Borylation of Arenes. *Chem. Lett.* **2019**, *48*, 1092–1100. [CrossRef]

44. Li, Y.; Wu, X.-F. Direct C–H Bond Borylation of (Hetero)Arenes: Evolution from Noble Metal to Metal Free. *Angew. Chem. Int. Ed.* **2020**, *59*, 1770–1774. [CrossRef] [PubMed]
45. Hall, D.G. *Boronic Acids: Preparation and Applications in Organic Synthesis and Medicine*; Wiley-VCH: Weinheim, Germany, 2005.
46. Obligacion, J.V.; Semproni, S.P.; Chirik, P.J. Cobalt-Catalyzed C(sp^2)-H Borylation. *J. Am. Chem. Soc.* **2014**, *136*, 4133–4136. [CrossRef] [PubMed]
47. Palmer, W.N.; Obligacion, J.V.; Pappas, I.; Chirik, P.J. Cobalt-Catalyzed Benzylic Borylation: Enabling Polyborylation and Functionalization of Remote, Unactivated C(sp^3)–H Bonds. *J. Am. Chem. Soc.* **2016**, *138*, 766–769. [CrossRef] [PubMed]
48. Schaefer, B.A.; Margulieux, G.W.; Small, B.L.; Chirik, P.J.J. Evaluation of Cobalt Complexes Bearing Tridentate Pincer Ligands for Catalytic C–H Borylation. *Organometallics* **2015**, *34*, 1307–1320. [CrossRef]
49. Furukawa, T.; Tobisu, M.; Chatani, N. Nickel-Catalyzed Borylation of Arenes and Indoles via C–H Bond Cleavage. *Chem. Commun.* **2015**, *51*, 6508–6511. [CrossRef] [PubMed]
50. Dombray, T.; Werncke, C.G.; Jiang, S.; Grellier, M.; Vendier, L.; Bontemps, S.; Sortais, J.-B.; Sabo-Etienne, S.; Darcel, C. Iron-Catalyzed C-H Borylation of Arenes. *J. Am. Chem. Soc.* **2015**, *137*, 4062–4065. [CrossRef]
51. Ros, A.; Fernández, R.; Lassaleta, J.M. Functional Group Directed C-H Borylation. *Chem. Soc. Rev.* **2014**, *43*, 3229–3243. [CrossRef]
52. Bisht, R.; Halder, C.; Hassan, M.M.M.; Hoque, M.E.; Chaturvedi, J.; Chattopadhya, B. Metal-Catalyzed C-H Bond Activation and Borylation. *Chem. Soc. Rev.* **2022**, *51*, 5042–5100. [CrossRef] [PubMed]
53. Itoh, H.; Kikuchi, T.; Ishiyama, T.; Miyaura, N. Iridium-catalyzed ortho-C–H Borylation of Aryl Ketones with Bis(pinacolato)diboron. *Chem. Lett.* **2011**, *40*, 1007–1008. [CrossRef]
54. Xue, C.; Luo, Y.; Teng, H.; Ma, Y.; Nishiura, M.; Hou, Z. Ortho-Selective C–H Borylation of Aromatic Ethers with Pinacol-borane by Organo Rare-Earth Catalysts. *ACS Catal.* **2018**, *8*, 5017–5022. [CrossRef]
55. Li, H.L.; Kuninobu, Y.; Kanai, M. Lewis Acid–Base Interaction-Controlled ortho-Selective C–H Borylation of Aryl Sulfides. *Angew. Chem. Int. Ed.* **2017**, *56*, 1495–1499. [CrossRef] [PubMed]
56. Li, H.-L.; Kanai, M.; Kuninobu, Y. Iridium/Bipyridine- Catalyzed ortho-Selective C–H Borylation of Phenol and Aniline Derivatives. *Org. Lett.* **2017**, *19*, 5944–5947. [CrossRef]
57. Chattopadhyay, B.; Dannatt, J.E.; Andujar-De Sanctis, I.L.; Gore, K.A.; Maleczka, R.E.; Singleton, D.A.; Smith, M.R. Ir-Catalyzed ortho-Borylation of Phenols Directed by Substrate–Ligand Electrostatic Interactions: A Combined Experimental/in Silico Strategy for Optimizing Weak Interactions. *J. Am. Chem. Soc.* **2017**, *139*, 7864–7871. [CrossRef] [PubMed]
58. Yamazaki, K.; Kawamorita, S.; Ohmiya, H.; Sawamura, M. Directed Ortho Borylation of Phenol Derivatives Catalyzed by a Silica-Supported Iridium Complex. *Org. Lett.* **2010**, *12*, 3978–3981. [CrossRef] [PubMed]
59. Sean, M.; Preshlock, S.M.; Ghaffari, B.; Peter, E.; Maligres, P.E.; Shane, W.; Krska, S.W.; Robert, E.; Maleczka, R.E., Jr.; Milton, R.; et al. High-Throughput Optimization of Ir-Catalyzed C–H Borylation: A Tutorial for Practical Applications. *J. Am. Chem. Soc.* **2013**, *135*, 7572–7582. [CrossRef] [PubMed]
60. Raphael, J.; Oeschger, R.J.; Larsen, M.A.; Bismuto, A.; Hartwig, J.F. Origin of the Difference in Reactivity between Ir Catalysts for the Borylation of C–H Bonds. *J. Am. Chem. Soc.* **2019**, *141*, 16479–16485. [CrossRef]
61. Boller, T.M.; Murphy, J.M.; Marko Hapke, M.; Tatsuo Ishiyama, T.; Miyaura, N.; Hartwig, J.F. Mechanism of the Mild Functionalization of Arenes by Diboron Reagents Catalyzed by Iridium Complexes. Intermediacy and Chemistry of Bipyridine-Ligated Iridium Trisboryl Complexes. *J. Am. Chem. Soc.* **2005**, *127*, 14263–14278. [CrossRef]
62. Ishiyama, T.; Jun Takagi, J.; Kousaku Ishida, K.; Norio Miyaura, N.; Anastasi, N.R.; Hartwig, J.E. Mild Iridium-Catalyzed Borylation of Arenes. High Turnover Numbers, Room Temperature Reactions, and Isolation of a Potential Intermediate. *J. Am. Chem. Soc.* **2002**, *124*, 390–391. [CrossRef] [PubMed]
63. Ochida, A.; Hara, K.; Ito, H.; Sawamura, M. Nonvolatile Me_3P-like P-Donor Ligand: Synthesis and Properties of 4-Phenyl-1-phospha-4-silabicyclo[2.2.2]octane. *Org. Lett.* **2003**, *5*, 2671–2674. [CrossRef] [PubMed]
64. Ochida, A.; Ito, S.; Miyahara, T.; Ito, H.; Sawamura, M. Electronically Tunable Compact Trialkylphosphines: SMAPs-bridged Bicyclic Phosphines. *Chem. Lett.* **2006**, *35*, 294–295. [CrossRef]
65. Kawamorita, S.; Ohmiya, H.; Hara, K.; Fukuoka, A.; Sawamura, M. Directed Ortho Borylation of Functionalized Arenes Catalyzed by a Silica-Supported Compact Phosphine–Iridium System. *J. Am. Chem. Soc.* **2009**, *131*, 5058–5059. [CrossRef] [PubMed]
66. Kawamorita, S.; Ohmiya, H.; Sawamura, M. Ester-Directed Regioselective Borylation of Heteroarenes Catalyzed by a Silica-Supported Iridium Complex. *J. Org. Chem.* **2010**, *75*, 3855–3858. [CrossRef] [PubMed]
67. Kawamorita, S.; Murakami, R.; Iwai, T.; Sawamura, M. Synthesis of Primary and Secondary Alkylboronates through Site-Selective C(sp^3)–H Activation with Silica-Supported Monophosphine–Ir Catalysts. *J. Am. Chem. Soc.* **2013**, *135*, 2947–2950. [CrossRef] [PubMed]
68. Konishi, S.; Kawamorita, S.; Iwai, T.; Steel, P.G.; Marder, T.B.; Sawamura, M. Site-Selective C–H Borylation of Quinolines at the C8 Position Catalyzed by a Silica-Supported Phosphane–Iridium System. *Chem. Asian. J.* **2014**, *9*, 434–438. [CrossRef]
69. Roosen, P.C.; Kallepalli, V.A.; Chattopadhyay, B.; Singleton, D.A.; Maleczka, R.E., Jr.; Smith, M.R., III. Outer-Sphere Direction in Iridium C–H Borylation. *J. Am. Chem. Soc.* **2012**, *134*, 11350–11353. [CrossRef] [PubMed]
70. Preshlock, S.M.; Plattner, D.L.; Maligres, P.E.; Krska, S.W.; Maleczka, R.E., Jr.; Smith, M.R., III. A Traceless Directing Group for C-H Borylation. *Angew. Chem. Int. Ed.* **2013**, *52*, 12915–12919. [CrossRef]
71. Bai, S.-T.; Bheeter, C.B.; Reek, J.N.H. Hydrogen Bond Directed *ortho*-Selective C-H Borylation of Secondary Aromatic Amides. *Angew. Chem. Int. Ed.* **2019**, *58*, 13039–13043. [CrossRef]

72. Hoque, M.M.; Hassan, M.M.M.; Chattopadhyay, B. Remarkably Efficient Iridium Catalysts for Directed C(sp^2)-H and C(sp^3)-H Borylation of Diverse Classes of Substrates. *J. Am. Chem. Soc.* **2021**, *143*, 5022–5037. [CrossRef] [PubMed]
73. Marcos-Atanes, D.; Vidal, C.; Navo, C.D.; Peccati, F.; Jiménez-Osés, G.; Mascareñas, J.L. Iridium-Catalyzed ortho-Selective Borylation of Aromatic Amides Enabled by 5-Trifluoromethylated Bipyridine Ligands. *Angew. Chem. Int. Ed.* **2023**, *62*, e202214510. [CrossRef]
74. Roering, A.J.; Hale, L.V.A.; Squier, P.A.; Ringgold, M.A.; Wiederspan, E.R.; Clark, T.B. Iridium-Catalyzed, Substrate-Directed C-H Borylation Reactions of Benzylic Amines. *Org. Lett.* **2012**, *14*, 3558–3561. [CrossRef] [PubMed]
75. Zou, X.; Zhao, H.; Li, Y.; Gao, Q.; Ke, Z.; Senmiao Xu, S. Chiral Bidentate Boryl Ligand Enabled Iridium-Catalyzed Asymmetric C(sp^2)–H Borylation of Diarylmethylamines. *J. Am. Chem. Soc.* **2019**, *141*, 5334–5342. [CrossRef] [PubMed]
76. Ros, A.; López-Rodríguez, R.; Estepa, B.; Álvarez, E.; Fernández, R.; Lassaletta, J.M. Hydrazone as the Directing Group for Ir-Catalyzed Arene Diborylations and Sequential Functionalizations. *J. Am. Chem. Soc.* **2012**, *134*, 4573–4576. [CrossRef]
77. Mao, S.; Yuan, B.; Wang, X.; Zhao, Y.; Wang, L.; Yang, X.-Y.; Chen, Y.-M.; Zhang, S.-Q.; Li, P. Triazene as the Directing Group Achieving Highly Ortho-Selective Diborylation and Sequential Functionalization. *Org. Lett.* **2022**, *24*, 3594–3598. [CrossRef]